Electro-Physical Properties of Niobia Columnlike Nanostructures via the Anodizing of Al/Nb Layers

A. Pligovka, A. Lazavenka, A. Zakhlebayeva
R&D Lab 4.10 "Nanotechnologies", Belarusian State University of Informatics and Radioelectronics,
Brovka Str. 6, Minsk 220013, Belarus, email: pligovka@bsuir.by

***Abstract*—**Two types of niobia columnlike nanostructures were synthesized by anodization, reanodization, and chemical etching of sputter-deposited Al/Nb metal layers. The morphological properties of synthesized niobia columnlike nanostructures were determined by means of scanning electron microscopy. The electro-physical characteristics of niobia columnlike nanostructures were investigated in two measurement schemes. Aluminum layers of thickness 500 nm were used as contact pads. The current–voltage I–U characteristic has a nonlinear and nonsymmetrical character. The rising of temperature leads to an increase of the current. This behavior may indicate a *p-n* or metal-semiconductor junction. The initial resistance at 23 °C was 60 and 120 kOhms, the specific resistance to the height of the columns was 87 and 116 kOhms·nm^{-1}, the calculated temperature coefficient of resistance appeared to be negative and rather low: -1.39×10^{-2} and -1.28×10^{-2} K^{-1} for the niobia columnlike nanostructures reanodized at 300 and 450 V, respectively.

I. Introduction

In the electronic industry, niobium oxide is considered to be a dielectric with high permittivity instead of silicon dioxide in semiconductor devices [1]. In niobia columnlike nanostructures (NCN) – oxygen system, the niobium element can be found in four different charge states: 0, 2+, 4+ and 5+. Generally, these charge states are related to the phases of metallic Nb and to the NbO, NbO_2 and Nb_2O_5 respectively [2]. Additionally, there exist numerous metastable oxides NbO_x with $0 < x < 1$ and $2.0 < x < 2.5$ as well as a multitude of Nb_2O_5 polymorphic modifications [3]. Niobium monoxide (NbO) presents typical metallic behaviour, and is widely regarded as a metal [4-6], with a resistivity of about 21 μΩ·cm at 25 °C [4, 6] that decreases with temperature down to 1.8 μΩ·cm at 4.2 K [6]. NbO is not used massively in any major technological application. However, the fact that niobium monoxide has improved properties, regarding the oxygen diffusion, in comparison with Nb, makes it a suitable candidate to niobium-based solid electrolytic capacitors [7–11]. Electrically, niobium dioxides (NbO_2) is characterized as being a semiconductor–metal transition, where this high temperature NbO_2 phase shows a typical metallic conductivity (c.a. 10^3 S/cm) [12]. Still, the tetragonal phase of NbO_2 is usually classified as being a *n*-type semiconductor with a small band gap (between 0.5 and 1.2 eV) [13] and an electrical resistivity in the order of 10^4 Ω·cm [5, 14-16]. Niobium pentoxide (Nb_2O_5) is the most thermodynamically stable state of the niobium–oxygen system. With a charge state of 5+ in Nb_2O_5, the electronic structure of the Nb atom is [Kr]$4d^0$, which means that all the 4*d* electrons are bonded to the O 2*p*-band, thus justifying the fact that Nb_2O_5 has a much lower electrical conductivity than the other niobium oxides [11]. It is possible to find several non-stoichiometric niobium oxides reported in literature. Essentially, these can be divided in two groups: one with stoichiometry between Nb and NbO, and other with stoichiometry between NbO_2 and Nb_2O_5. Overall, Marucco [17] concluded that the only stable phases of niobium oxides with a stoichiometry between $NbO_{2.4}$ and $NbO_{2.5}$ are Nb_2O_5, $Nb_{12}O_{29}$ and $Nb_{25}O_{62}$ where such variations in stoichiometry are possible to occur, and can be interpreted as single or doubly charged oxygen vacancies in their structure, resulting in significant variations of the electrical resistance [2]. Thus, oxide niobium systems can exhibit from conductor to dielectric properties, depending on the ratios of oxide phases. Although, NCN were first formed more than six years ago [18], investigation of the electro-physical properties of such nanostructures hasn't been carried out yet.

In the present work, NCN have been synthesized via sputter-deposition and anodizing of thin-film samples Al/Nb metal bilayer. These NCN were evaluated as a semiconductor through the fabrication of metal–NCN–metal elements, whose characteristics were studied in a wide range of temperatures, voltages and currents. The morphological properties of synthesized NCN were determined by means of scanning electron microscopy (SEM).

II. Experimental

Two-layer Al/Nb (1500/300 nm) systems sputter-deposited on 100 mm Si wafer (*n*-type, 4", 500 μm thick, 4–40 Ω·cm) were used as a starting substrate. The Si wafer was anodized in specially designed cylindrical two electrode cell made of polytetrafluoroethylene. It was placed horizontally in the cell and a polytetrafluoroethylene ring was fastened tightly to the aluminium surface, so that only a surface area of 67 cm^2 was available for anodizing. The programmable power supply Keysight N5751A was used as the anodization unit.

The Al/Nb bilayer, the whole thickness of the upper aluminum layer was anodically consumed (oxidized), down to the niobium layer, so that the thickness of the porous anodic alumina (PAA) formed was expected to be 2175 nm, because, at the selected anodizing conditions, the relevant value of Pilling–Bedworth ratio (PBR) for Al/Al_2O_3 was reported to be 1.45 [19]. Anodizing the Al/Nb samples was performed in two consecutive steps: first, potentiostatic anodizing aluminum

978-1-5386-5336-4/18/$31.00 ©2018 IEEE

was carried out in 0.4 mol·dm^{-3} aqueous solution of oxalic acid at 37 V beyond some 15 min, with a steady-state current of 450 mA, until the aluminum metal was fully oxidized. Then the process was supported into a voltage-stabilization mode, at which the current began to decay. During this step the alumina barrier layer touches the niobium, local oxidation occurs through the alumina pores and continues until an array of nanosized niobium oxide hillocks formed at the interface and described in more details in a previous work [20]. Second, the specimen is reanodized in 1% citric acid solution by sweeping the voltage at a constant rate of 0.1 V·s^{-1} from zero to a more anodic value (hereafter referred to as reanodizing voltage). As reported before [21], high voltage reanodizing of an initially anodized Al/Nb bilayer sample consumes the remaining niobium metal locally under the pores with the formation of niobium oxide nanocolumns penetrating into the pores. The extent to which the pores are filled by growing niobium oxide depends strikingly on the reanodizing voltage value. One of the approaches to the formation of planar NCN is to remove some of the porous alumina by chemically etching to the tops of the columns. The etching time is determined by the diameter of the oxide cell and is independent of the total thickness of the porous oxide. To slightly release the column tops from the 2175 nm PAA matrix with oxide cell size 90 nm, the alumina film may be etch-cleaned in a hot mixture of phosphoric and chromic acids (hereafter the selective etchant [22]) for 360 s. Complete removal of PAA matrix for SEM was carried out in aqueous solution of 50% phosphoric acid at 50 °C during 600 s.

For fabricating measuring elements, a 500 nm thick aluminum layer was sputter-deposited over the surface of the anodized samples. Arrays of top square contact pads, of graded sizes from 1×1 mm, were then formed from the upper aluminum layer via photolithography and chemical etching. The distance between the contact pads was 1 mm. Two types of NCN were used. The first type of NCN was reanodized at 300 V (NCN_{300}). The second type of NCN was reanodized 450 V (NCN_{450}). The measurement scheme of electro-physical characteristics of elements is presented in Fig. 1.

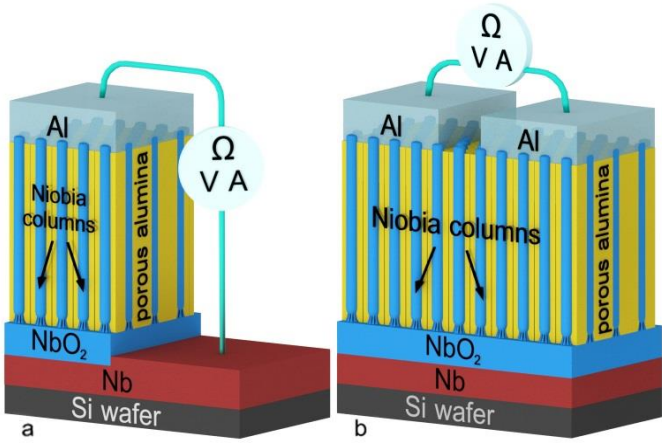

Fig. 1. Schematic 3-D views of (a) first and (b) second types architectures employed for measuring electrical characteristics of the niobia columnlike nanostructures.

The first measurement scheme had a structure: the upper contacts pad 1×1 mm – NCN – the lower contact pad was an unoxidized underlayer of niobium (Fig. 1a). The second measurement scheme had a structure: upper contacts pad 1×1 mm – NCN – upper contacts pad 1×1 mm (Fig. 1b). The following parameters were measured in Keysight 34401: current–voltage I–U characteristics at voltage increasing stepwise from -20 to 20 V at temperatures in the range from 20 to 80 °C, current–voltage I–U cacharacteristic for breakdown and resistance at temperatures in the range from 20 to 80 °C. Temperature coefficient of resistance (TCR) was determined from the measured resistance values in the temperature range 20–80 °C, as described elsewhere [23].

NCN were observed in a Hitachi S-4800 operated at 10-15 kV. In the latter case, a gold layer, about 3 nm in thickness, was evaporated over the specimens to reduce the charging effects.

III. Results and Discussion

Fig. 2 shows the surface and transverse faults of the two NCN types obtained as described in the experimental section using SEM.

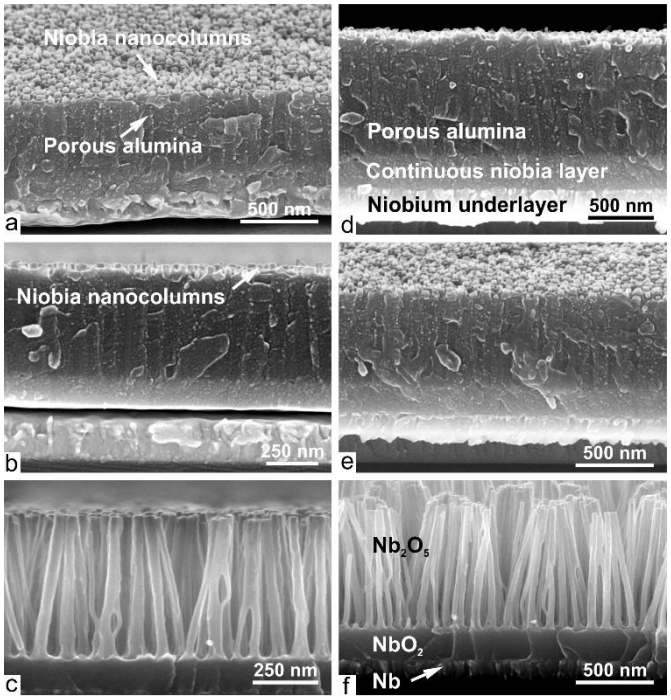

Fig. 2. Scanning electron microscope images of the niobia columnlike nanostructures on Si-substrate formed by sequential anodization at 37 V in 0.4 mol·dm^{-3} $H_2C_2O_4$ with subsequent reanodization in 1% $C_6H_8O_7$ at 23 °C (a-c) at 300 V and (d-f) at 450 V. The images shown in (c and f) were obtained after the alumina layer had been dissolved away ("alumina-free" samples).

The presence of nanosized columns passing through the film and reaching the top of the alumina film is also confirmed by SEM of the specimen fractures in Fig. 2a, b and d, e. Three layers can be distinguished in the SEM image: columns of anodic niobia protruding from PAA, an upper layer comprising the columns penetrating the pores and a lower

layer of continuous niobia lying between the upper film layer and the residual niobium layer. The niobium metal is a polycrystalline with mainly rod-like grains typically developed by the magnetron method. All of the NCN had the following sequence of layers (Fig. 2), down-up: Si wafer – niobium metal – continuous niobia – columns of anodic niobia penetrating the PAA – columns of anodic niobia protruding from PAA.

From Fig. 2, the NCN have a different thickness, consisting of regularly distributed alumina cells with a diameter of ~90 nm, and pores, of ~15 nm in diameter, each containing nanocolumns about 43 nm in the average diameter. The height of columns is about 518 nm for NCN_{300} and 766 nm for NCN_{450}. The thickness of continues niobia layer is about 142 nm for NCN_{300} and 225 nm for NCN_{450}. The top of the nanocolumns niobia above the surface of the film is about ~40 nm. The displacement of niobium columns from PAA is due to the selective etching process. The etchant penetrates into the pores and etching proceeds not only on the surface of the NCN but also in the pores in all directions. The thickness of the barrier layer is 40 nm, which corresponds to the height at which the columns of niobia from PAA protrude. The measured film parameters are summarized in Table 1. Minor deviations of the parameters in the tables can be caused by the measurement error and the formation method.

Table 1. Morphological parameters of the niobia columnlike nanostructures reanodized at 300 V and 450 V.

Morphological parameters	NCN_{300}	NCN_{450}
PAA thickness, nm	518	766
Average cell diameter of PAA, nm	90	90
Average pore diameter, nm	15	15
Niobium metal thickness, nm	234	222
Continuous niobia thickness (H_{low}), nm	142	225
Height of niobia columns (H_{up}), nm	551	811
Columns protruding from PAA, nm	39	40
Average diameter of niobia columns, nm	43	43

Fig. 3a displays the current–voltage I–U characteristics for NCN_{300} with the first type measurement scheme. The current flowed along the way: contact pad – nanocolumns – continues layer – niobium underlayer – electrode. The current–voltage I–U curves have a nonlinear and nonsymmetrical character. The rising of temperature leads to an increase of the current. This behavior may indicate a *p-n* or metal-semiconductor junction.

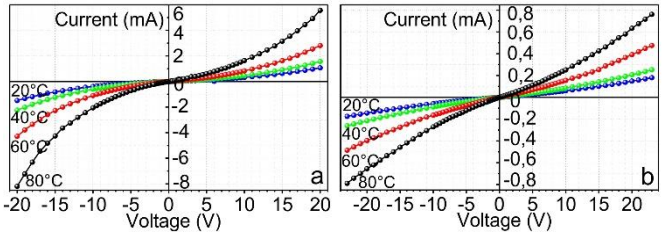

Fig. 3. The current–voltage I–U characteristics at voltage increasing stepwise from -20 to 20 V at temperatures in the range from 20 to 80 °C of the niobia columnlike nanostructures reanodized (a) at 300 V and connected the first scheme, (b) at 450 V and connected the second scheme.

The current–voltage I–U characteristics for NCN_{450} were measured according to the second scheme (Fig. 3b). There are current–voltage I–U curves that have a nonlinear but symmetrical character. With this type of connection, it can be assumed that two junctions are connected in series. This behavior of the current–voltage I–U characteristic confirms the semiconductor nature of NCN.

Fig. 4a shows the current–voltage I–U characteristic for breakdown voltage for the NCN_{450} with the first type measurement scheme at 23 °C. As it can be seen from Fig. 4a, the I-U characteristic has an exponential distribution. When the voltage reached 65-70 V the current starts to rise sharply and breakdown occurs. The repeated measurement of the resistance of broken contacts gives the value of 2-6 Ohms, which corresponds to the resistance of metal-insulator-metal capacitors after a breakdown [24].

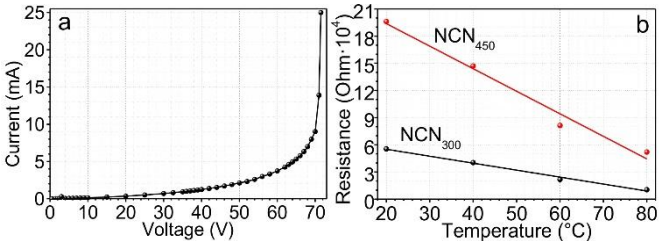

Fig. 4. (a) The current–voltage I–U curve for breakdown at voltage increasing stepwise from 0 to 70 V at 23 °C of the niobia columnlike nanostructures reanodized at 450 V and connected the first scheme. (b) Temperature dependence of resistance of the niobia columnlike nanostructures reanodized at 300 V with connected the first scheme, at 450 V with connected the second scheme.

Fig. 4b displays the resistance at temperatures in the range from 20 to 80 °C for the NCN_{300} with the first measurement scheme and the NCN_{450} with the second measurement scheme. All the NCN prepared in this study were characterized by negative and linear TCR. The initial resistance for NCN_{300} and NCN_{450} were 60 and 120 kOhms, respectively. Morphological parameters from the table and the initial resistance R make it possible to estimate the specific resistance R_H to the height of the columns as

$$R_H = \frac{R}{H_{low} + H_{up}}, \qquad (1)$$

H_{low}, H_{up} were presented in the Table 1 and described in [25]. R_H has for NCN_{300} is 87 kOhms·nm^{-1}, and for NCN_{450} is 116 kOhms·nm^{-1}. The calculated TCR appears to be negative and rather low: -1.39×10^{-2} K^{-1} and -1.28×10^{-2} K^{-1} for NCN_{300} and NCN_{450}, respectively.

IV. CONCLUSIONS

In our work we managed to form two types of niobia columnlike nanostructures applying to a blend of anodization, reanodization, and chemical etching of sputter-deposited Al/Nb metal layers. Due to the smart formation approach, the film growth proceeds smoothly, without dielectric breakdown

and destructive field crystallization and physical defects, which are usual attributes for anodic and thermal oxide growth on niobium, limiting the techniques available for well-controlled preparation of niobia columnlike nanostructures. Two types of niobia columnlike nanostructures were used. The first type of niobia columnlike nanostructures was reanodized at 300 V. The second type of niobia columnlike nanostructures was reanodized 450 V. The height of niobia columns was 551 and 811 nm, the diameter was 43 nm, and the thickness of continues niobia layer was about 142 and 225 nm. The thickness of the barrier layer is about 40 nm, which corresponds to the height at which the columns of the niobia from porous anodic alumina protrude. The electro-physical characteristics of the niobia columnlike nanostructures were investigated in two measurement schemes. Aluminum layers of thickness 500 nm were used as contact pads. The current–voltage I–U curve has a nonlinear and nonsymmetrical character. The rising of temperature leads to an increase of the current. This behavior may indicate a *p-n* or metal-semiconductor junction. The initial resistance was 60 and 120 kOhms, the specific resistance to the height of the columns was 87 and 116 kOhms·nm^{-1}, the calculated temperature coefficient of resistance appears to be negative and rather low: -1.39×10^{-2} and -1.28×10^{-2} K^{-1} for the niobia columnlike nanostructures reanodized at 300 and 450 V, respectively.

ACKNOWLEDGMENT

Andrei Pligovka thanks the Mobility Scheme for Targeted People-to-People-Contacts under project R-ZUFm-39628 for the opportunity to present the work at the 18th IEEE International Conference on Nanotechnology. The authors gratefully acknowledge contribution of Ms. Alexandra Metla of BSUIR for her help with computer-aided modeling.

REFERENCES

[1] S. Venkataraj, D. Severin, S. H. Mohamed, J. Ngaruiya, O. Kappertz, & M. Wuttig, "Towards understanding the superior properties of transition metal oxynitrides prepared by reactive DC magnetron sputtering," Thin Solid Films, vol. 502, iss. 1–2 pp. 228–234, Apr. 2006. [Online]. Available: http://dx.doi.org/10.1016/j.tsf.2005.07.280

[2] C. Nico, T. Monteiro, & M. P. F. Graça, "Niobium oxides and niobates physical properties: review and prospects," Progress in Materials Science, vol. 80, pp. 1–37, Jul. 2016. [Online]. Available: http://dx.doi.org/10.1016/j.pmatsci.2016.02.001

[3] A. Mozalev, R. M. Vázquez, C. Bittencourt, D. Cossement, F. Gispert-Guirado, E. Llobet, & H. Habazaki, "Formation–structure–properties of niobium-oxide nanocolumn arrays via self-organized anodization of sputter-deposited aluminum-on-niobium layers," Journal of Materials Chemistry C, vol. 2, iss. 24, pp. 4847–4860, Apr. 2014. [Online]. Available: http://dx.doi.org/10.1039/c4tc00349g

[4] E. R. Pollard, Electronic properties of niobium monoxide, thesis, MIT, Cambridge, Massachusetts, USA, 1968.

[5] E. Z. Kurmaev, A. Moewes, O. G. Bureev, I. A. Nekrasov, V. M. Cherkashenko, M. A. Korotin, & D. L. Ederer, "Electronic structure of niobium oxides," Journal of alloys and compounds, vol. 347, iss. 1–2, 213–218, Dec. 2002. [Online]. Available: http://dx.doi.org/10.1016/S0925-8388(02)00765-X

[6] J. K. Hulm, C. K. Jones, R. A. Hein, & J. W. Gibson, "Superconductivity in the TiO and NbO systems," Journal of Low Temperature Physics, vol. 7, iss. 3–4, pp. 291–307, May 1972. [Online]. Available: http://dx.doi.org/10.1007/BF00660068

[7] Y. Qiu, D. Smyth, & J. Kimmel, "The stabilization of niobium-based solid electrolyte capacitors," Active and passive electronic components, vol. 25, iss. 2, pp. 201–209, 2002. DOI: 10.1080/0882751021000001591

[8] T. Karnik, "Ceramic powder for use in forming an anode of an electrolytic capacitor," G.B. Patent 2 454 049 (A), 2009.

[9] T. Karnik, "Doped ceramic powder for use in forming capacitor anodes," U.S. Patent 7 760 487, Jul. 20, 2010.

[10] C. Nico, M. R. N. Soares, J. Rodrigues, M. Matos, R. Monteiro, M. P. F. Graça, ... & T. Monteiro, "Sintered NbO powders for electronic device applications," The Journal of Physical Chemistry C, vol. 115, iss. 11, pp. 4879–4886, Mar. 2011. [Online]. Available: http://dx.doi.org/10.1021/jp110672u.

[11] M. R. N. Soares, S. Leite, C. Nico, M. Peres, A. J. S. Fernandes, M. P. F. Graça, ... & F. M. Costa, "Effect of processing method on physical properties of Nb_2O_5," Journal of the European Ceramic Society, vol. 31, iss. 4, pp. 501–506, Apr. 2011. [Online]. Available: https://doi.org/10.1016/j.jeurceramsoc.2010.10.024

[12] R. F. Janninck, & D. H. Whitmore, "Electrical conductivity and thermoelectric power of niobium dioxide," Journal of Physics and Chemistry of Solids, vol. 27, iss. 6–7, pp. 1183–1187, June–July 1966. [Online]. Available: http://dx.doi.org/10.1016/0022-3697(66)90094-1

[13] A. O'Hara, T. N. Nunley, A. B. Posadas, S. Zollner, & A. A. Demkov, "Electronic and optical properties of NbO_2," Journal of Applied Physics, vol. 116, iss. 21, p. 213705, Dec. 2014. [Online]. Available: https://doi.org/10.1063/1.4903067

[14] D. S. Rimai, & R. J. Sladek, "Pressure dependences of the elastic constants of semiconducting NbO_2 at 296 K," Physical Review B, vol. 18, iss. 6, p. 2807, Sept. 1978. [Online]. Available: http://dx.doi.org/10.1103/PhysRevB.18.2807.

[15] Y. Zhao, Z. Zhang, & Y. Lin, "Optical and dielectric properties of a nanostructured NbO2 thin film prepared by thermal oxidation," Journal of Physics D: Applied Physics, vol. 37, no. 24, p. 3392, Dec. 2004. [Online]. Available: https://doi.org/10.1088/0022-3727/37/24/006

[16] R. F. Janninck, & D. H. Whitmore, "Electrical conductivity and thermoelectric power of niobium dioxide," Journal of Physics and Chemistry of Solids, vol. 27, iss. 6-7, pp. 1183–1187, Jun. 1966. [Online]. Available: https://doi.org/10.1016/0022-3697(66)90094-1

[17] J. F. Marucco, "Electrical resistance and defect structure of stable and metastable phases of the system $Nb_{12}O_{29}$–Nb_2O_5 between 800 and 1100 °C," The Journal of Chemical Physics, vol. 70, no. 2, pp. 649–654, 1979. [Online]. Available: https://doi.org/10.1063/1.437545

[18] A. Mozalev, H. Habazaki, & J. Hubálek, "The superhydrophobic properties of self-organized microstructured surfaces derived from anodically oxidized Al/Nb and Al/Ta metal layers," Electrochimica Acta, vol. 82, pp. 90–97, May 2012. [Online]. Available: https://doi.org//10.1016/j.electacta.2012.05.065

[19] V. Surganov, A. Mozalev, & I. Mozaleva, "Volume growth of anodic oxide and rate of electrochemical anodization of aluminium in oxalic acid electrolyte," Russ. J. Appl. Chem, vol. 68, pp. 1638–1642, 1995.

[20] A. Mozalev, M. Sakairi, I. Saeki, and H. Takahashi, "Nucleation and growth of the nanostructured anodic oxides on tantalum and niobium under the porous alumina film," Electrochimica Acta, vol. 48, iss. 20–22, pp. 3155–3170, Sept. 2003. [Online]. Available: https://doi.org/10.1016/S0013-4686(03)00345-1

[21] A. Pligovka, A. Zakhlebayeva, & A. Lazavenka, "Niobium oxide nanocolumns formed via anodic alumina with modulated pore diameters," Journal of Physics: Conference Series, vol. 987, no. 1, p. 012006, Mar. 2018. DOI :10.1088/1742-6596/987/1/012006

[22] G.C.Wood, in: J.W. Diggle (Ed.), Oxides and Oxide Films, vol. 2, New York, Marcell Dekker, 1987, p. 41.

[23] L. I. Maissel, & R. Glang, Handbook of thin film technology, vol. 2, New York, McGraw-Hill, 1970, p. 21.

[24] A. N. Pligovka, A. N. Luferov, R. F. Nosik, & A. M. Mozalev, "Dielectric characteristics of thin film capacitors based on anodized Al/Ta layers," In Proc. Int. Crimean Conf. Microwave and Telecommunication Technology (CriMiCo), Sept. 2010, pp. 880–881. DOI: 10.1109/CRMICO.2010.5632734

[25] A. Mozalev, A. J. Smith, S. Borodin, A. Plihauka, A. W. Hassel, M. Sakairi, & H. Takahashi, "Growth of multioxide planar film with the nanoscale inner structure via anodizing Al/Ta layers on Si,"

Electrochimica Acta, vol. 54, iss. 3, pp. 935–945, Jan. 2009. [Online]. Available: https://doi.org/10.1016/j.electacta.2008.08.030